Analytical and Bioanalytical Chemistry
https://doi.org/10.1007/s00216-018-1108-5

RESEARCH PAPER

Monitoring dynamic release of intracellular hydrogen peroxide through a microelectrode based enzymatic biosensor

Hang Zhang[1] · Jun Ruan[1] · Weiwei Liu[1] · Xuerui Jiang[1] · Tianyu Du[1] · Hui Jiang[1] · Pasquarelli Alberto[2] · Kay-Eberhard Gottschalk[2] · Xuemei Wang[1]

Received: 2 February 2018 / Revised: 25 March 2018 / Accepted: 24 April 2018

Abstract

A high sensitive and selective hydrogen peroxide (H_2O_2) biosensor was fabricated on the basis of reduced hemoglobin (Hb) and single-walled carbon nanotubes (SWCNTs) for detecting the release of H_2O_2 from living HepG2 cancer cells in the process of the in situ biosynthesis of ZnO quantum. The modification of carbon fiber microelectrode (CFME) was carried out by physical adsorption. By the scanning electron microscopy (SEM) and energy-dispersive X-ray spectroscopy (EDS), the dense cover of surface and successful immobilization were characterized. Electrochemical investigation demonstrates that the as-prepared modified microelectrode showed a quasi-reversible process toward the reduction of H_2O_2, which exhibited a linear range from 0.51 to 10.6 μM, with a limit of detection of 0.23 μM. This microelectrode biosensor was applied for the quantification of the change of H_2O_2 concentration released from HepG2 cells through the in situ biosynthesis of ZnO quantum dots, which was further confirmed by the fluorescence staining.

Keywords Microelectrode · Biosensor · Hydrogen peroxide · Intracellular ROS

Introduction

Reactive oxygen species (ROS) known as one of significant intracellular signaling molecules [1], mainly regulating potential biological process, including DNA damage, proteins synthesis, and cell apoptosis [2, 3]. The excessive amount of ROS usually leads to oxidative stress that causes various pathological such as cancer [4], Alzheimer's disease [5, 6], Parkinson's disease [7, 8], and heart disease [9]. Therefore, the measurement of intracellular ROS can lead to a deeper cognition of the clinical manifestations of the enhanced ROS concentration and provide an opportunity to elucidate its biological effect. Hydrogen peroxide (H_2O_2), as a particularly interesting component of ROS, has been widespread concerned due to its importance for the growth, development, and health of living organisms [10, 11]. Imbalances in H_2O_2 generation can lead to oxidative stress that cause DNA damage and inhibit the activity of cellular enzymes to influence apoptosis and proliferation, and promote tumorigenesis [12]. Therefore, it is important to explore the quantitative and selective detection of H_2O_2 and measurement of its dynamic release process from living cells in order to understand the role of H_2O_2 in various pathological conditions, though this is often hindered by the difficulties associated with the determination of concentrations of intracellular H_2O_2 due to the limited permeability across the plasma membrane [13]. Therefore, a fast and accurate method for the detection of intracellular H_2O_2 will have profound applications in clinical, environmental analysis, and other fields [14]. Although some analytical methods have been employed for the detection of H_2O_2 such as chemiluminescence [15], fluorescence [16], and spectrophotometry [17], they are often restricted to the requirements of tracers or instable chemical probes. Meanwhile, the detection of H_2O_2 by electrochemical sensors has attracted much attention in various research areas due to their simplicity, rapidity, and high spatial resolution since H_2O_2 is an electroactive molecule

✉ Xuemei Wang
xuewang@seu.edu.cn

[1] State Key Laboratory of Bioelectronics, National Demonstration Center for Experimental Biomedical Engineering Education, School of Biological Science and Medical Engineering, Southeast University, Nanjing 210096, China

[2] Institute of Experimental Physics, Ulm University, Albert Einstein Allee 45, 89069 Ulm, Germany

Published online: 24 May 2018

[18]. Moreover, the sizes of electrochemical biosensors can be fabricated extremely small so that high spatial resolution measurement can be obtained [19].

For the monitoring of intracellular H_2O_2, carbon fiber microelectrode (CFME) was widely used due to their tip size comparable with cells size (i.e., normally 20 μm in diameter) so that it can readily detect the activity in the cellular microenvironments with minimized damage. Meanwhile, biocompatibility and outstanding electrical properties make CFME an ideal tool for the real-time measurements [20]. CFME has been reported to safely realize the in vivo H_2O_2 measurement. Sanford et al. [21] fabricated a bare CFME for the detection of H_2O_2 in rat striatum slices by the method of fast scan cyclic voltammetry (FSCV). Besides, it was found that the sensitivity for H_2O_2 detection could be improved through modification of the naked CFME with horseradish peroxidase (HRP) [22], Nafion [23], carbon nanotubes [24], graphene [25, 26], metal nanoparticles [27], etc.

In the past decades, enzyme-based electrochemical biosensors for the detection of H_2O_2 have received considerable attention through the immobilization of enzymes or protein because of their remarkable selectivity [28]. Hence, an enzymatic sensor is highly appreciated for the high sensitive and selective detection of intracellular H_2O_2 by the strategy of direct electron transfer, without requirements for an intermediary mediator between the electrode and substrate. Single-walled carbon nanotubes (SWCNTs) have attracted great interest in the field of biosensors due to their outstanding properties such as high electrical conductivity, high surface area, and excellent chemical stability [29]. The increasing sensitivity of SWCNTs-based biosensor is attributed to the facilitation of electron transfer from biomolecules to electrodes and the mitigation of the surface fouling effects by biomolecules [30, 31]. Meanwhile, hemoglobin (Hb) as one of the renowned heme proteins has four iron-centered porphyrin structures with reversible redox activity [32, 33]. The redox potential change depends on the microenvironment surrounding the heme groups, allowing its wide used for construction of various biosensors [34]. Therefore, we used the SWCNTs as a robust scaffold for the immobilization of Hb to construct an enzyme-based biosensor. It is quite attractive for the measurement of intracellular H_2O_2 based on the modified CFME.

Here, in order to explore the possibility of using electrochemical method for detecting the H_2O_2 in the process of the in situ biosynthesis of ZnO quantum dots based on the recent report that Fe^{2+} and Zn^{2+} could target some diseased sites and provide a multiple mode self-imaging of cancerous cells via the formation of multi-functionalized nanoclusters including fluorescent ZnO quantum dots and iron oxide clusters that was involving in the participation of H_2O_2 in the cell [35]. Therefore, quantitative detection of intracellular H_2O_2 is of great value in elaborating its regulation in the relevant biological process. Based on the above considerations, a sensitive hydrogen peroxide (H_2O_2) microelectrode biosensor was fabricated through the modification of the reduced Hb and SWCNTs, whose sensitivity and selectivity were electrochemically characterized, and further applied for the measurements of H_2O_2 dynamic release process from HepG2 cells (Scheme 1). The excellent performance of the as-prepared biosensor was further confirmed by intracellular fluorescence staining in the process of in situ biosynthetic ZnO quantum dots.

Materials and methods

Chemicals and instrumentation

Hb and hexadecyltrimethyl ammonium bromide (CTAB) were purchased from Sigma-Aldrich. SWCNTs (purity > 75 wt%, 1–2 nm in outer diameter, 5–15 μm in length) were bought from Macklin (Shanghai, China) and used as received. All other reagents were purchased from Sinopharm Chemical Reagen Co., Ltd. (Shanghai, China). Carbon fiber (diameter of 7 μm) was purchased from Goodfellow Co. (Oxford, UK). Glass capillary (inner diameter of 0.9 mm, the outer diameter of 1.1 mm) was obtained from West China Medical Instrument Inc. (Chengdu, China). All solutions used in the experiments were prepared with deionized water (18.2 MΩ cm, Millipore). To eliminate dissolved oxygen, the solutions were purged with high purity nitrogen (99.99%, gas supply Inc., CETC 14, Nanjing) for 30 min. The nitrogen atmosphere was maintained over the solutions during the electrochemical measurements.

A scanning electron microscope (SEM; Hitachi Ltd., Japan) were used to characterize the morphology. EDS

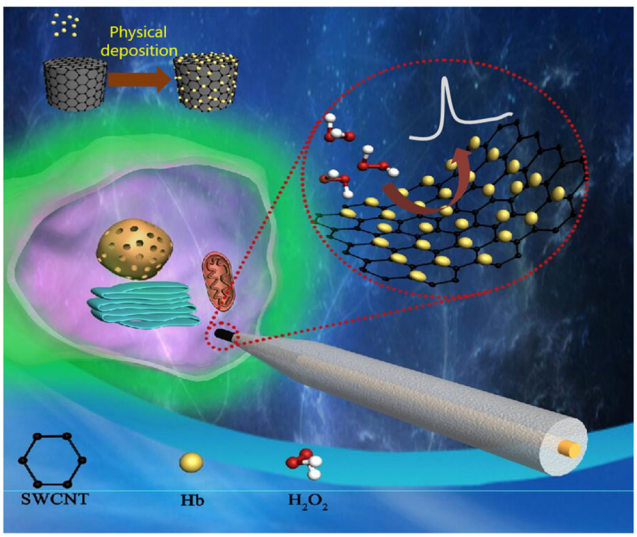

Scheme 1 Schematic illustration of the as-prepared modified CFME for measuring the H_2O_2 released from the stimulated HepG2 cells

analysis was carried out by using a SEM equipped with an energy-dispersive X-ray detector. All electrochemical measurements were carried out by using a 3-electrode system including a modified CFME, a platinum wire (CHI Incorporation, USA), and an Ag/AgCl wire (CHI Incorporation, USA) as the working, counter, and a reference electrode, respectively. A computer-controlled CHI660A electrochemical workstation (CHI Incorporation, USA) was used for all electrochemical experiments. A confocal laser scanning microscope (Nikon C-2, Japan) was applied to confirm the successful staining of the cells.

Fabrication and modification of CFME

Single carbon fiber was attached to a copper wire with conducive silver adhesives. After drying, it was inserted into a glass capillary (length of 10 cm and inter diameter of 0.5 mm) until the carbon fiber was located in the middle of the capillary. After that, the capillary was pulled with the microelectrode puller to expose the carbon fiber. Then, the copper wire was fixed with paraffin in the capillary. The length of the protruded carbon fiber was cut to 100 μm with a scalpel under an inverted microscope for an initial CFME. Before electrochemical etching, the tip was cleaned by dipping in acetone for about 30 s to dissolve extra paraffin. Then, the CFME pretreatment for electrochemical activation was performed in a 0.5 M sulfuric acid solution by potential cycling in the potential range from − 1.0 to + 1.0 V at a scan rate of 50 mV s^{-1} until a stable cyclic voltammogram was obtained.

The microelectrode modification was promoted as described below. In brief, 3 mg of SWCNTs were ultrasonically dispersed in 1 mL aqueous solution of CTAB (10 mg mL^{-1}) for 1 h to obtain a homogeneous black suspension. Then, 10 mg of Hb was dissolved in the above suspension under stirring for 10 min. The CFME was soaked in 1 mL mixture under an infrared lamp. After the solvent evaporation, a uniform Hb/SWCNTs film was formed on the surface of CFME.

Cell culture and electrochemical detection

The HepG2 cells (human liver carcinoma cells) were purchased from Shanghai Institute of Biological Sciences, Chinese Academy of Science. The cells were cultured in a Dulbecco's modified eagle medium (DMEM) replenished with 10% FBS and 1% streptomycin/penicillin at 37 °C with 5% CO_2 under a 95% humidified atmosphere. After a convenient incubation time, the cells were equally divided into three groups and respectively treated as follows: (a) treatment with 20 μM zinc gluconate and 10 μM ferrous chloride, (b) treatment with 20 μM zinc gluconate, and (c) control group without any further treatment. After 12 h incubation, the cells were washed three times with PBS. To capture H_2O_2 molecules released from target cells, the modified CFME was held in the proximity of the HepG2 cells. When the baseline was stabilized, camptothecin (CPT) was injected to the solution, which can motivate cells generation of H_2O_2 [36], and have no interference to the detection of H_2O_2. The fast diffusion of H_2O_2 molecules toward the microelectrode makes it possible to realize the accurate quantification study. At the potential of − 0.35 V (vs Ag/AgCl), the amperometric current response was recorded at modified CFME. The experiments were conducted in the deoxygenated PBS at 37 °C. Every measurement was repeated at least three times during all experimental studies.

Fluorescence staining measurement

The procedure of cells preparation was the same as described above. Before detection, the target cells of each group were stained with specific fluorescent dyes of DCFH-DA for about 30 min. The cells samples were cultured in glass bottom cell dishes before imaging. Afterwards, the medium was removed, and the adherent cells were rinsed and washed three times with PBS (pH = 7.4). Finally, the whole cell fluorescent images were recorded by a confocal laser scanning microscope.

Results and discussion

SEM characterization

SEM images were utilized to investigate the surface morphology of the as-prepared CFME. As shown in Fig. 1a, it is evident that the bare CFME surface was smooth and clean. In comparison with the bare CFME surface, the modification of SWCNTs provides the sheets which largely increase the specific surface area for immobilization of Hb. As shown in Fig. 1b, a dense surface covering is observed. Besides, the EDS observation indicates the co-existence of N and Fe elements since the bare microelectrodes contains only C element [37], confirming the existence of Hb (Fig. 1c).

Electrochemical behavior of the modified CFME

Cyclic voltammetry was applied to characterize the electrochemical behavior of modified CFME in 0.1 M deoxygenated PBS (pH = 7.4) (Fig. 2a). After the incorporation of SWCNTs and Hb onto the surface of CFME, a pair of well-defined redox peaks and an enhanced current signal were observed, with an cathodic peak potential (E_{pc}) at about − 0.35 V and anodic peak potential (E_{pa}) at about − 0.27 V, as shown in Fig. 2a, c. These observations illustrate that the peak potential separation was about 80 mV, indicating a quasi-reversible process [38]. This electrochemical behavior has been attributed to Fe(II)/Fe(III) redox couple in Hb, while the enhanced current signal was attributed to the enlarged interface area of modified CFME with

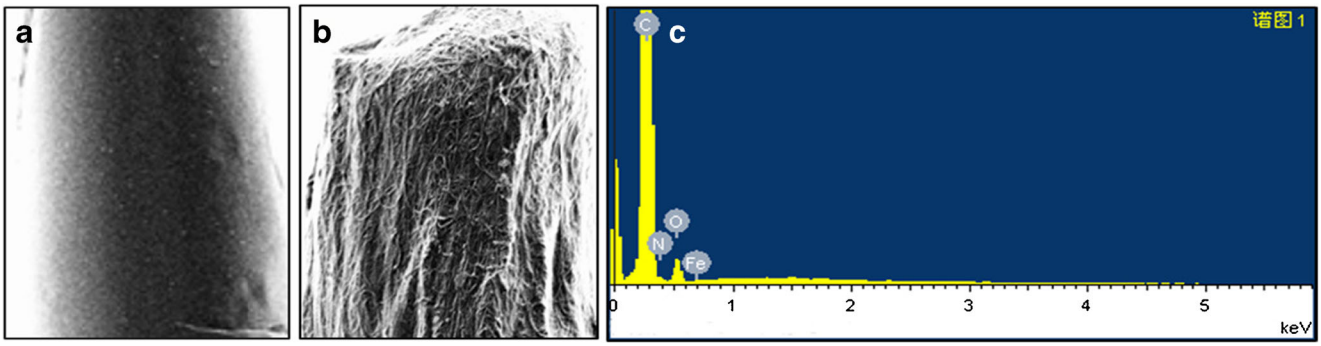

Fig. 1 The SEM images of **a** bare CFME and **b** the as-prepared modified CFME. **c** The EDS observation on the surface of this modified CFME

SWCNTs, which provided many effective paths for direct electron transfer between Hb and CFME [39]. Meanwhile, as shown in Fig. 2b, it is observed that anodic and cathodic peak currents increase linearly as the scan rates varied from 100 to 500 mV s^{-1}, with a correlation coefficient of 0.99, suggesting a typical surface-controlled process [40]. The above results show that Hb was adsorbed effectively and reliably at the surface of SWCNTs and the electron transfer was mediated efficiently from Hb to CFME. Figure 2c, d shows the responses to the presence and absence of 0.5 mM H_2O_2 on bare and modified CFME, respectively. Upon addition of H_2O_2, the cathode current of the modified CFME obviously increased, while the bare CFME showed little changes. Furthermore, under the identical experimental conditions, the specific response of the as-prepared biosensor to the same concentration of H_2O_2 was more than 100 times larger when compared with the CFME

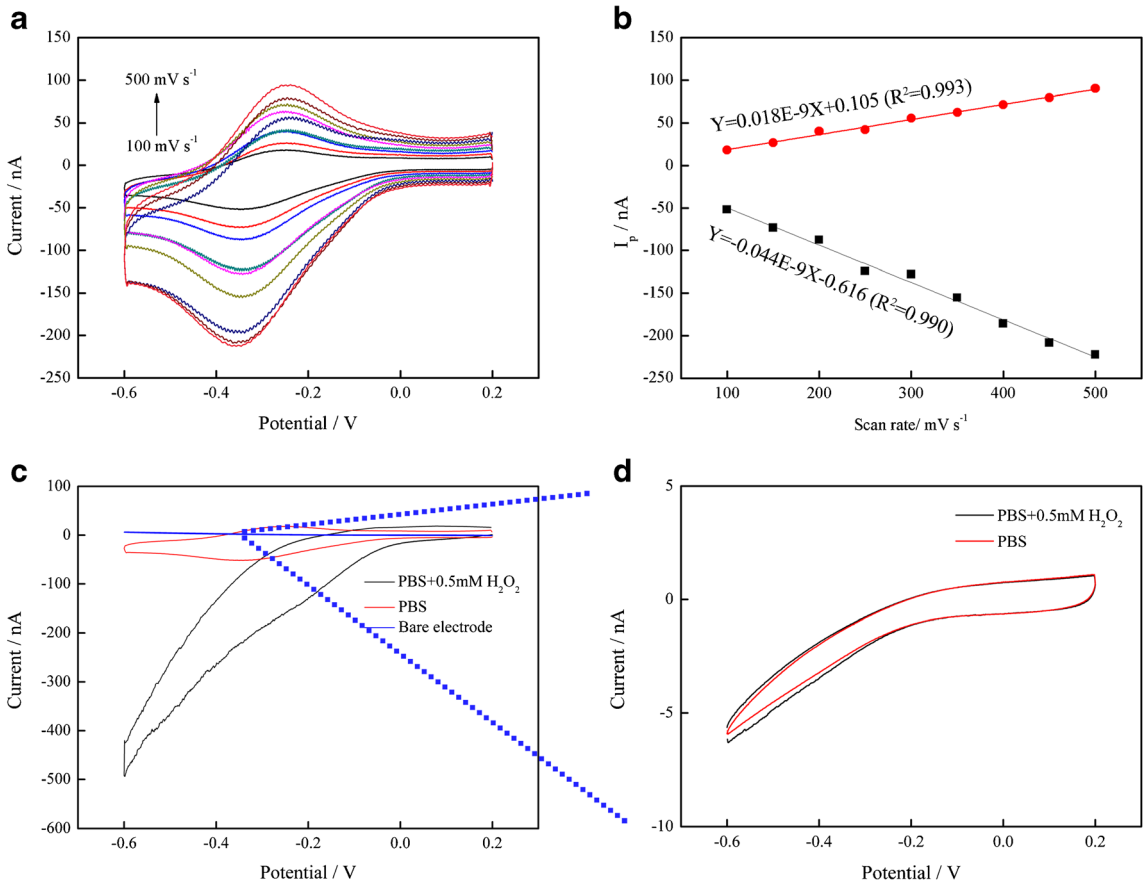

Fig. 2 **a** Cyclic voltammetry of CFME modified with Hb/SWCNT in 0.1 M deoxygenated PBS (pH = 7.4) at a scan rate of 100 to 500 mV s^{-1}. **b** Plot of current anodic (black squares) and cathodic (red round dots) peak current vs scan rate. Cyclic voltammetry of **c** modified CFME and **d** bare CFME in 0.1 M deoxygenated PBS (pH = 7.4) in the absence and presence of 0.5 mM H_2O_2. Scan rate = 50 mV s^{-1}

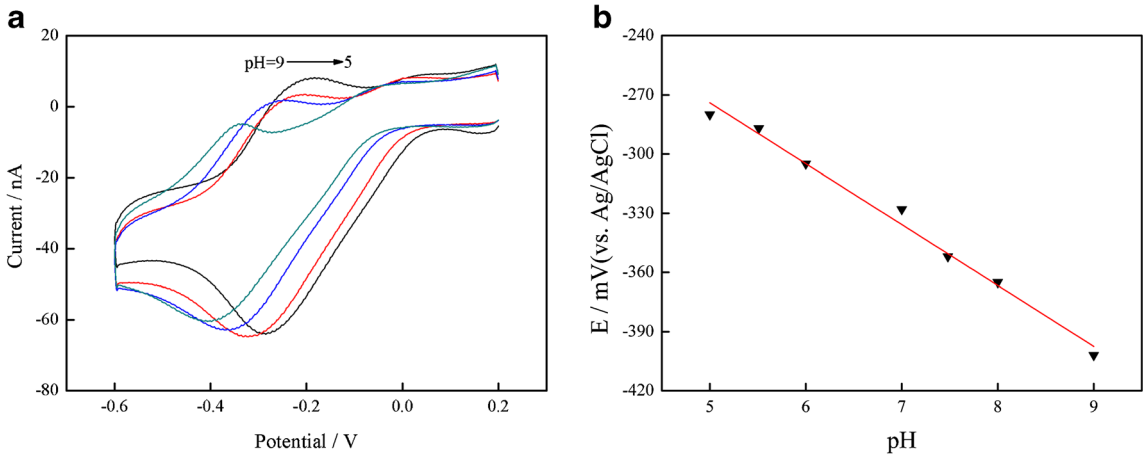

Fig. 3 **a** Influence of pH on cyclic voltammograms of the as-prepared CFME, the pH values are 9, 8, 7, 5 respectively (from left to right). **b** The relationship of the formal potential (E) with pH, scan rate = 100 mV s^{-1}

modified with SWCNT alone (data not shown), indicating that the as-prepared modified CFME was more sensitive to H_2O_2 change and applicable to detect the relevant H_2O_2 released from the stimulated HepG2.

Meanwhile, the pH of buffer solution was an important factor for the direct electrochemistry of the modified CFME. As shown in Fig. 3a, with the increase of pH, a negative shift of both reduction and oxidation peak potentials was observed. In the pH range from 5.0 to 9.0, all the cyclic voltammograms showed a quasi-reversible redox process. A good linear relationship was found between the formal potential and pH value as shown in Fig. 3b. The slope value was calculated as − 30.4 mV pH^{-1}, which was smaller than the theoretical value of 57.6 mV pH^{-1} for one-electron transfer coupled with one-proton transportation [41]. It may be attributed to the protonation of *trans*-ligands or the protonation of water molecule

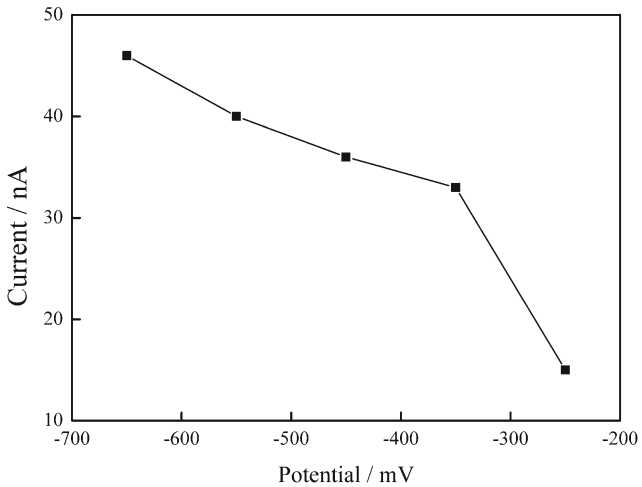

Fig. 4 Influence of applied potential on amperometric response of the as-prepared CFME in the presence of 3 μM H_2O_2

and central iron. Therefore, based on the consideration of performance from the above observational data, we have selected pH = 7.4 phosphate buffer for the subsequent working media solution. For biosensor, it is also a very significant factor to work under right circumstance of potential. We investigated the influence of applied potential on response of the biosensor to H_2O_2 by the method of amperometric detection. Figure 4 displays the cathodic peak current at different applied potential. The results show as the voltage increases from − 250 to − 650 mV the steady-state current gradually increases, which is similar to that of cyclic voltammetric characterization. In this study, − 0.35 V was chosen as the working potential for the amperometric determination of H_2O_2, where the risk for interfering reactions of other electroactive species was minimized [42].

Figure 5a illustrates the dependence of the electrochemical catalysis current on the concentration change of H_2O_2. The as-prepared biosensor could achieve the maximum peak current within 4 s. It was found that the apparent steady-state current had a good linear relationship with the corresponding H_2O_2 concentration in the range of 0.51–10.6 μM ($R^2 = 0.998$) having sensitivity of 9.95 μA mM^{-1} with a limit of detection of 0.23 μM (S/N = 3). The apparent Michalis-Menten constant ($K_{m,app}$), which is an indicator of the affinity between enzymes and substrates, can be calculated from the improved formula of the Lineweaver-Burk equation [43]:

$$1/I_{ss} = \left(1/I_{max}\right) + \left(K_{m,app}/I_{max}\right)1/C$$

Here, I_{ss} is the steady-state current, C is the bulk concentration of the substrate, and I_{max} is the maximum current. While Fig. 5b shows the linear relationship of $Y = 0.73758X + 0.36492$ ($R^2 = 0.9987$), the value of $K_{m,app}$ can

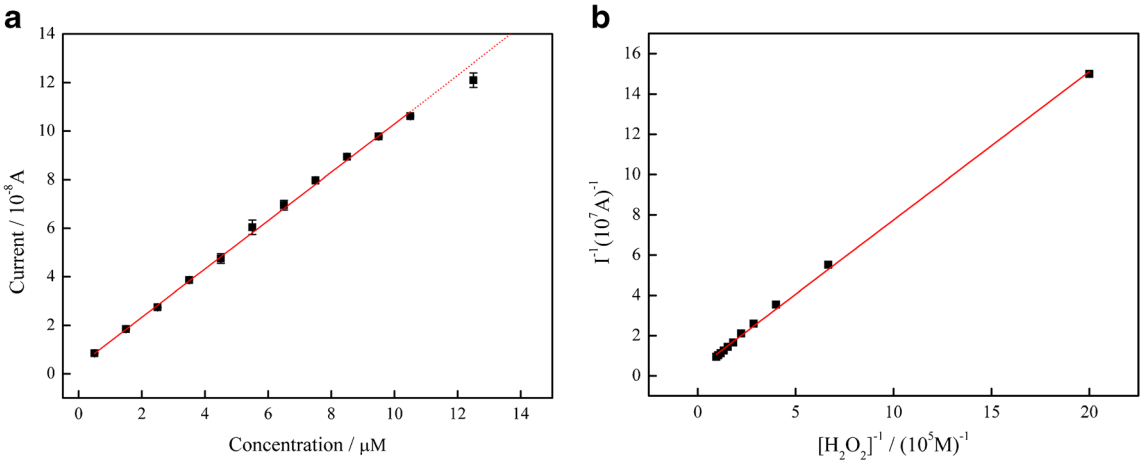

Fig. 5 **a** Calibration curve of the faradic current to the concentration of H_2O_2 in air-saturated 0.01 M PBS buffer. **b** The Lineweaver-Burk plot. Applied potential: − 0.35 V vs. Ag/AgCl sat. KCl. Error bars are the standard error of the mean ($n = 5$ electrodes)

be obtained as 20.2 μM. The value is smaller than some previous reports [44, 45]. A comparison of detection potential, linear range, and detection limit for the enzymatic biosensor with other H_2O_2 biosensors reported in the literature are shown in Table 1, indicating that some analytical parameters are comparable and even better than those reported in previous literatures. Meanwhile, since the intracellular H_2O_2 from the biological stimulation could reach micromolar level, the as-prepared CFME could readily realize the detection of intracellular H_2O_2 [46].

Reproducibility and stability of the modified CFME

Reproducibility and storage stability are quite essential for H_2O_2 biosensor. The relative standard deviation (RSD) was 2.35% for eight successive measurements. For the reproducibility of six independently as-prepared CFME, an acceptable relative standard deviation of 3.11% was observed for the sensitivity to H_2O_2. When the as-prepared CFME was not in use, it was stored in PBS (pH = 7.4) at 4 °C. The storage stability of the as-prepared biosensor was studied by measuring the amperometric response to 0.01 mM H_2O_2 once a day. The results showed an excellent stability that the response decreased to about 95% of its initial value in the first 3 days and still remained about 86% of the initial value in 10 days. These results may be attributed to the stability of SWCNT and good biological activity of Hb in CTAB. Thus, the modified CFMEs have been excellent reproducibility and stability.

Interference from electroactive substances

Ascorbic acid (AA) [47] and glutathione (GSH) [48] in cells are the main electrochemically active substances which may interfere with cellular analysis. Figure 6 illustrates the amperometric response of the as-prepared CFME upon successive addition of H_2O_2 (1.5 μM), GSH (15 μM), AA (15 μM), H_2O_2 (1.5 μM) in 0.1 M PBS, respectively. It was found that both of AA and GSH yielded little current response at this

Table 1 Comparison of the performance of various hydrogen peroxide sensors

Electrode materials	Detection potential (V)	Linear range (μM)	Detection limit (μM)
Pt nanoparticles/HRP [22]	− 0.3 (vs. Ag/AgCl)	0.35–3600	0.35
Carbon nanotube/Pt nanoparticle [24]	− 0.1 (vs. Ag/AgCl)	160–11,500	55
Graphene/Pt-nanocomposite [25]	− 0.08 (vs. Ag/AgCl)	0.5–3475	0.2
Graphene/CuI [26]	0 (vs. Ag/AgCl)	0.5–3000	0.2
Se/Pt nanocomposite [27]	0 (vs. Ag/AgCl)	10–15,000	3.1
DNA/Hb [28]	− 0.75 (vs. Ag/AgCl)	10–120	0.4
Nafion/Nano-CaCO3/Hb film [44]	− 0.28 (vs. SCE)	8.0–240	5
Hb/single-wall carbon nanotube (this work)	− 0.35 (vs. Ag/AgCl)	0.51–10.6	0.23

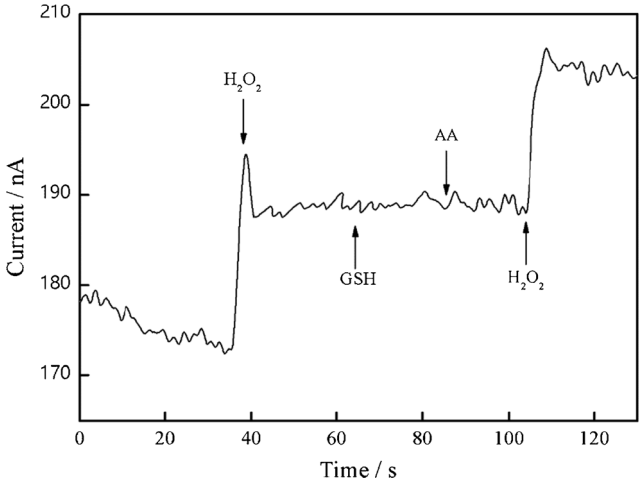

Fig. 6 Amperometric response of the as-prepared CFME to successive addition of 1.5 μM H_2O_2, 15 μM GSH, 15 μM AA, and a second 1.5 μM H_2O_2. Applied potential: − 0.35 V vs. Ag/AgCl sat KCl

modified CFME under the applied potential. The current response of H_2O_2 was not affected in the presence of the other electroactive compounds. These observations demonstrate that the as-prepared CFME could have good specificity and selectivity to detect intracellular H_2O_2 released from the stimulated cells.

The detection of H_2O_2 release from the stimulated HepG2 cells

The detection of H_2O_2 released from HepG2 cells was performed to explore the bio-application of the as-prepared CFME. Our previous studies found that the biosynthesized nanoclusters could be formed from the relevant interaction between Zn^{2+} and hydroxyl radicals from H_2O_2 via the Fenton reaction, which could accelerate the process of the

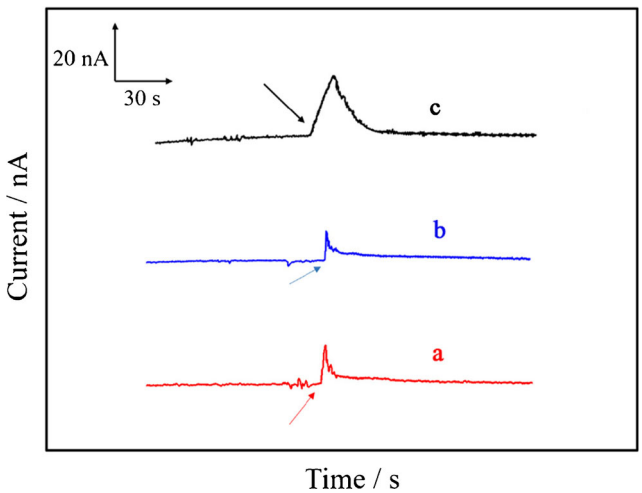

Fig. 7 Amperometric responses of the as-prepared modified CFME for H_2O_2 released from HepG2 cells with different pretreatment through adding CPT: cells treated with **a** Zn^{2+}, **b** Zn^{2+}/Fe^{2+}, and **c** control

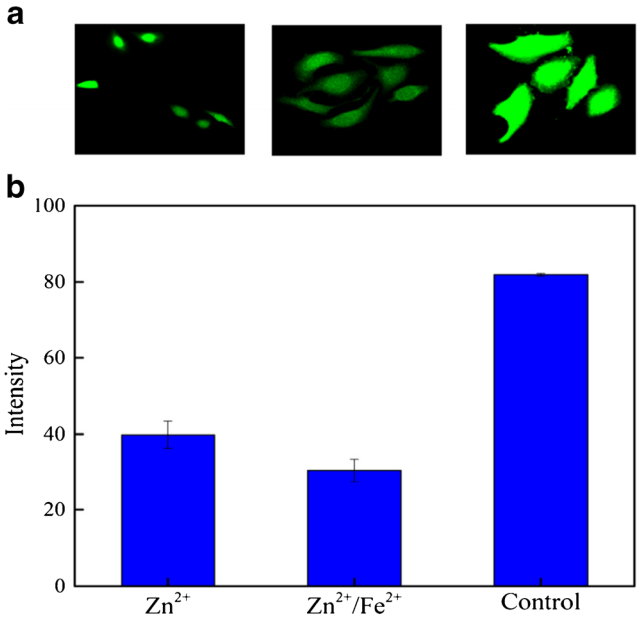

Fig. 8 **a** Confocal fluorescence images of intracellular H_2O_2 staining, **b** corresponding quantitative analysis

in situ biosynthetic ZnO quantum dots [35]. However, quantitative evaluation of intracellular H_2O_2 changes remains to be further exploited. The dynamic H_2O_2 release from the HepG2 cells which had different pretreatments were measured in this study by using the as-prepared modified CFME, where the HepG2 cells were stimulated by injecting CPT to induce H_2O_2 generation. Figure 7 illustrates instantaneous current before and after injection of CPT to the culture media of HepG2 cells with various pretreatments. It is obvious that H_2O_2 could readily cross the lipid bilayer of membrane from the target cells [49]. The rapid change of relevant peak current could be obviously observed, which is consistent with that previously reported [50]. It is noted that control group (c) has the maximum current change of about 21.6 nA, which was corresponding to 1.98 μM of H_2O_2. In the treatment groups, the results show 11.78 (a) and 8.84 nA (b) for the target HepG2 cells treated with Zn^{2+} and Zn^{2+}/Fe^{2+}, respectively, with a corresponding concentration of 1.08 and 0.81 μM of H_2O_2. These observations suggest that H_2O_2 has been heavily consumed during the in situ biosynthesis process of ZnO quantum dots in target HepG2 cells. In addition, the subsequently decreased current indicates that H_2O_2 released from the stimulated cells diffuses into the solution. Moreover, it is evident that the addition of exotic ferrous ion apparently promotes the process of the in situ biosynthesized ZnO quantum dots and thus consumes much more intracellular H_2O_2. The relevant variations of H_2O_2 released from different treatment groups could be attributed to Fenton reaction, where Fe^{2+} and H_2O_2 react to hydroxyl ions that also promote the reaction with Zn^{2+}, which is consistent with those previously reported [35, 51].

Fluorescence study of intracellular H_2O_2 staining

Based on the above observations, the fluorescence staining study was further explored to confirm the above studies of different groups. The traditional staining method of DCFH-DA is suitable for assessing the general intracellular ROS status, though it only gives qualitative results, whereas the electrochemical sensor could easily quantify the real-time data like the release of electrochemically active species versus time. As shown in Fig. 8, after dying with DCFH-DA, the intensity of green fluorescence was measured to indicate the intracellular H_2O_2 level. The results show that the ration of fluorescence intensity between the control group and the treatment groups for the target HepG2 cells treated with Zn^{2+} and Zn^{2+}/Fe^{2+} is 1.83 and 2.44, respectively, indicating that that H_2O_2 has been heavily consumed during the in situ biosynthesis process of ZnO quantum dots in target HepG2 cell, and the addition of exotic ferrous ion apparently promotes the process of the in situ biosynthesized ZnO quantum dots, thus consuming much more intracellular H_2O_2. These observations are highly consistent with the electrochemical results about the intracellular concentration of H_2O_2.

Conclusions

In summary, we have explored a new strategy in this contribution to fabricate an enzymatic biosensor through fabricating the reduced Hb and SWCNTs modified CFME. Our studies demonstrate that the as-prepared modified CFME exhibited high sensitivity, selectivity, and affinity for H_2O_2 detection. The linear range from 0.51 to 10.6 μM was observed for this enzymatic biosensor, with a relevant detection limit of 0.23 μM. The relatively low detection limit and high sensitivity will be applicable for detecting H_2O_2 dynamic release from the stimulated living cells. More importantly, we have introduced the enzymatic biosensor to detect H_2O_2 of the in situ biosynthetic ZnO quantum dots, and attempted to preliminarily study the concentration change of H_2O_2 in this process, which was further confirmed with fluorescence staining. These results not only provide a basis for the future work for studying its kinetic process, but raise the possibility to use the microelectrode-based enzyme biosensor to monitor in real-time other important biological process in future biomedical applications.

Acknowledgements This work is supported by the National High-tech R&D Program and National Key Research & Development Program of China (Nos. 2017YFA0205301), and the National Natural Science Foundation of China (Nos. 91753106, 81325011, 21327902).

Compliance with ethical standards

Conflict of interest The authors declare that they have no conflict of interest.

References

1. Valko M, Leibfritz D, Moncol J, Cronin MT, Mazur M, Telser J. Free radicals and antioxidants in normal physiological functions and human disease. Int J Biochem Cell Biol. 2007;39(1):44–84.
2. Chang H, Wang X, Shiu K-K, Zhu Y, Wang J, Li Q, et al. Layer-by-layer assembly of graphene, au and poly (toluidine blue O) films sensor for evaluation of oxidative stress of tumor cells elicited by hydrogen peroxide. Biosens Bioelectron. 2013;41:789–94.
3. Roberts JG, Hamilton KL, Sombers LA. Comparison of electrode materials for the detection of rapid hydrogen peroxide fluctuations using background-subtracted fast scan cyclic voltammetry. Analyst. 2011;136(17):3550–6.
4. Valko M, Izakovic M, Mazur M, Rhodes CJ, Telser J. Role of oxygen radicals in DNA damage and cancer incidence. Mol Cell Biochem. 2004;266(1–2):37–56.
5. Behl C, Davis J, Lesley R, Schubert D. Hydrogen peroxide mediates amyloid B protein toxicity. Cell. 1994;77(6):817–27.
6. Sultana R, Butterfield DA. Role of oxidative stress in the progression of Alzheimer's disease. J Alzheimers Dis. 2010;19(1):341–53.
7. Weisskopf M, O'reilly E, Chen H, Schwarzschild M, Ascherio A. Plasma urate and risk of Parkinson's disease. Am J Epidemiol. 2007;166(5):561–7.
8. Brieger K, Schiavone S, Miller FJ Jr, Krause K-H. Reactive oxygen species: from health to disease. Swiss Med Wkly. 2012;142: w13659.
9. Pryor WA. Vitamin E and heart disease: basic science to clinical intervention trials. Free Radic Biol Med. 2000;28(1):141–64.
10. Miller EW, Chang CJ. Fluorescent probes for nitric oxide and hydrogen peroxide in cell signaling. Curr Opin Chem Biol. 2007;11(6):620–5.
11. Paulsen CE, Carroll KS. Orchestrating redox signaling networks through regulatory cysteine switches. ACS Chem Biol. 2009;5(1): 47–62.
12. Matés JM, Segura JA, Alonso FJ, Márquez J. Intracellular redox status and oxidative stress: implications for cell proliferation, apoptosis, and carcinogenesis. Arch Toxicol. 2008;82(5):273–99.
13. Miller EW, Dickinson BC, Chang CJ. Aquaporin-3 mediates hydrogen peroxide uptake to regulate downstream intracellular signaling. Proc Natl Acad Sci. 2010;107(36):15681–6.
14. Yao S, Xu J, Wang Y, Chen X, Xu Y, Hu S. A highly sensitive hydrogen peroxide Amperometric sensor based on MnO_2 nanoparticles and Dihexadecyl hydrogen phosphate composite film. Anal Chim Acta. 2006;557(1–2):78–84.
15. Wang K, Liu Q, Wu X-Y, Guan Q-M, Li H-N. Graphene enhanced electrochemiluminescence of Cds nanocrystal for H_2O_2 sensing. Talanta. 2010;82(1):372–6.
16. Wen F, Dong Y, Feng L, Wang S, Zhang S, Zhang X. Horseradish peroxidase functionalized fluorescent gold nanoclusters for hydrogen peroxide sensing. Anal Chem. 2011;83(4):1193–6.
17. Nogueira RFP, Oliveira MC, Paterlini WC. Simple and fast spectrophotometric determination of H_2O_2 in photo-Fenton reactions using Metavanadate. Talanta. 2005;66(1):86–91.
18. Wightman RM. Probing cellular chemistry in biological systems with microelectrodes. Science. 2006;311(5767):1570–4.
19. Forster RJ. Microelectrodes: new dimensions in electrochemistry. Chem Soc Rev. 1994;23(4):289–97.

20. Huffman ML, Venton BJ. Carbon-Fiber microelectrodes for in vivo applications. Analyst. 2009;134(1):18–24.
21. Sanford AL, Morton SW, Whitehouse KL, Oara HM, Lugo-Morales LZ, Roberts JG, et al. Voltammetric detection of hydrogen peroxide at carbon fiber microelectrodes. Anal Chem. 2010;82(12):5205–10.
22. Wu Z, Chen L, Shen G, Yu R. Platinum nanoparticle-modified carbon fiber ultramicroelectrodes for mediator-free biosensing. Sensors Actuators B Chem. 2006;119(1):295–301.
23. Ross AE, Venton BJ. Nafion–Cnt coated carbon-Fiber microelectrodes for enhanced detection of adenosine. Analyst. 2012;137(13):3045–51.
24. Wen Z, Ci S, Li J. Pt nanoparticles inserting in carbon nanotube arrays: nanocomposites for glucose biosensors. J Phys Chem C. 2009;113(31):13482–7.
25. Zhang Y, Bai X, Wang X, Shiu K-K, Zhu Y, Jiang H. Highly sensitive graphene–Pt nanocomposites Amperometric biosensor and its application in living cell H_2O_2 detection. Anal Chem. 2014;86(19):9459–65.
26. Li C, Liu X, Zhang Y, Chen Y, Du T, Jiang H, et al. A novel nonenzymatic biosensor for evaluation of oxidative stress based on nanocomposites of graphene blended with cui. Anal Chim Acta. 2016;933:66–74.
27. Li Y, Zhang J-J, Xuan J, Jiang L-P, Zhu J-J. Fabrication of a novel nonenzymatic hydrogen peroxide sensor based on Se/Pt nanocomposites. Electrochem Commun. 2010;12(6):777–80.
28. Kafi A, Yin F, Shin H-K, Kwon Y-S. Hydrogen peroxide biosensor based on DNA–Hb modified gold electrode. Thin Solid Films. 2006;499(1–2):420–4.
29. Patolsky F, Weizmann Y, Willner I. Long-range electrical contacting of redox enzymes by Swcnt connectors. Angew Chem Int Ed. 2004;43(16):2113–7.
30. Guiseppi-Elie A, Lei C, Baughman RH. Direct Electron transfer of glucose oxidase on carbon nanotubes. Nanotechnology. 2002;13(5):559.
31. Yao Y, Shiu K-K. Electron-transfer properties of different carbon nanotube materials, and their use in glucose biosensors. Anal Bioanal Chem. 2007;387(1):303–9.
32. Yagati AK, Choi JW. Protein based electrochemical biosensors for H2o2 detection towards clinical diagnostics. Electroanalysis. 2014;26(6):1259–76.
33. Ren QQ, Yuan XJ, Huang XR, Wen W, Zhao YD, Chen W. In vivo monitoring of oxidative burst on Aloe under salinity stress using hemoglobin and single-walled carbon nanotubes modified carbon fiber ultramicroelectrode. Biosens Bioelectron. 2013;50:318–24.
34. Chen W, Cai S, Ren QQ, Wen W, Zhao Y-D. Recent advances in electrochemical sensing for hydrogen peroxide: a review. Analyst. 2012;137(1):49–58.
35. Du T, Zhao C, ur Rehman F, Lai L, Li X, Sun Y, et al. Rapid and multimodal in vivo bioimaging of cancer cells through in situ biosynthesis of Zn&Fe nanoclusters. Nano Res. 2017;10(8):2626–32.
36. Simizu S, Takada M, Umezawa K, Imoto M. Requirement of caspase-3 (-like) protease-mediated hydrogen peroxide production for apoptosis induced by various anticancer drugs. J Biol Chem. 1998;273(41):26900–7.
37. Fan Y, Yang H, Liu X, Zhu H, Zou G. Preparation and study on radar absorbing materials of nickel-coated carbon fiber and flake graphite. J Alloys Compd. 2008;461(1):490–4.
38. Song S, Dong S. Spectroelectrochemistry of the quasi-reversible reduction and oxidation of hemoglobin at a methylene blue adsorbed modified electrode. J Electroanal Chem Interfac. 1988;253(2):337–46.
39. Yan Y, Zheng W, Zhang M, Wang L, Su L, Mao L. Bioelectrochemically functional Nanohybrids through co-assembling of proteins and surfactants onto carbon nanotubes: facilitated electron transfer of assembled proteins with enhanced faradic response. Langmuir. 2005;21(14):6560–6.
40. Lu Q, Hu S, Pang D, He Z. Direct electrochemistry and electrocatalysis with hemoglobin in water-soluble quantum dots film on glassy carbon electrode. Chem Commun. 2005;20:2584–5.
41. Meites L, Delahay P. Polarographic techniques. J Electrochem Soc. 1966;113(5):124C.
42. Zhang XW, Qiu QF, Jiang H, Zhang FL, Liu YL, Amatore C, et al. Real-time intracellular measurements of Ros and Rns in living cells with single core–shell nanowire electrodes. Angew Chem Int Ed. 2017;56(42):12997–3000.
43. Kamin RA, Wilson GS. Rotating ring-disk enzyme electrode for biocatalysis kinetic studies and characterization of the immobilized enzyme layer. Anal Chem. 1980;52(8):1198–205.
44. Sun W, Rf G, Jiao K. Electrochemistry and electrocatalysis of a Nafion/Nano-Caco3/Hb film modified carbon ionic liquid electrode using Bmimpf6 as binder. Electroanalysis. 2007;19(13):1368–74.
45. Wang H, Guan R, Fan C, Zhu D, Li G. A hydrogen peroxide biosensor based on the bioelectrocatalysis of hemoglobin incorporated in a Kieselgubr film. Sensors Actuators B Chem. 2002;84(2–3):214–8.
46. He R, Tang H, Jiang D. Chen H-y. Electrochemical visualization of intracellular hydrogen peroxide at single cells. Anal Chem. 2016;88(4):2006–9.
47. Davey MW, Montagu MV, Inzé D, Sanmartin M, Kanellis A, Smirnoff N, et al. Plant L-ascorbic acid: chemistry, function, metabolism, bioavailability and effects of processing. J Sci Food Agric. 2000;80(7):825–60.
48. Chen J, He Z, Liu H, Cha C. Electrochemical determination of reduced glutathione (Gsh) by applying the powder microelectrode technique. J Electroanal Chem. 2006;588(2):324–30.
49. Jones R, Morice A. Hydrogen peroxide—an intracellular signal in the pulmonary circulation: involvement in hypoxic pulmonary vasoconstriction. Pharmacol Ther. 2000;88(2):153–61.
50. Gorman A, McGowan A, Cotter TG. Role of peroxide and superoxide anion during tumour cell apoptosis. FEBS Lett. 1997;404(1):27–33.
51. Enami S, Sakamoto Y, Colussi AJ. Fenton chemistry at aqueous interfaces. Proc Natl Acad Sci. 2014;111(2):623–8.